Development 129, 1-12 (2002)
Printed in Great Britain © The Company of Biologists Limited 2002
DEV5936

Morphogenetic pattern formation during ascidian notochord formation is regulative and highly robust

Edwin M. Munro[1,2,*] and Garrett Odell[1]

[1]Department of Zoology, University of Washington, Seattle, WA 98195, USA
[2]Friday Harbor Labs, Friday Harbor, WA 98250, USA
*Author for correspondence at address 1 (e-mail: munroem@u.washington.edu)

Accepted 5 October 2001

SUMMARY

The ascidian notochord forms through simultaneous invagination and convergent extension of a monolayer epithelial plate. Here we combine micromanipulation with time lapse and confocal microscopy to examine how notochord-intrinsic morphogenetic behaviors and interactions with surrounding tissues, determine these global patterns of movement. We show that notochord rudiments isolated at the 64-cell stage divide and become motile with normal timing; but, in the absence of interactions with non-notochordal tissues, they neither invaginate nor converge and extend. We find that notochord formation is robust in the sense that no particular neighboring tissue is required for notochord formation. Basal contact with either neural plate or anterior endoderm/lateral mesenchyme or posterior mesoderm are each alone sufficient to ensure that the notochord plate forms and extends a cylindrical rod. Surprisingly, the axis of convergent extension depends on the specific tissues that contact the notochord, as do other patterns of cell shape change, movement and tissue deformation that accompany notochord formation. We characterize one case in detail, namely, embryos lacking neural plates, in which a normal notochord forms but by an entirely different trajectory. Our results show ascidian notochord formation to be regulative in a fashion and to a degree never before appreciated. They suggest this regulative behavior depends on a complex interplay between morphogenetic tendencies intrinsic to the notochord plate and instructive and permissive interactions with surrounding tissues. We discuss mechanisms that could account for these data and what they imply about notochord morphogenesis and its evolution within the chordate phylum.

Key words: Ascidian, Notochord, Pattern formation, Morphogenesis

INTRODUCTION

Understanding how global patterns of tissue movement and deformation emerge from the combined activities of many individual cells remains a central unsolved problem in developmental biology. We consider this problem in the context of ascidian notochord formation, in which simultaneous invagination and convergent extension transforms a monolayer plate of 40 cells into a cylindrical rod (Munro and Odell, 2002). Active crawling of basolateral notochord cell edges across the faces of their adjacent neighbors accompanies this transformation and probably drives it. Basolateral crawling is biased both within the plane of the notochord plate and along the apical-basal axis in a way that could account for both invagination and convergent extension. But the source of this bias is unknown.

Experimental and theoretical studies have identified many possible sources of patterned cellular behavior within tissues and these fall into two classes. First, pre-existing cytoplasmic asymmetries and/or spatial pre-patterns in the expression of "morphoregulatory" genes could determine spatial patterns of intrinsic motile and adhesive behavior before any morphogenetic movements occur. For example, pre-existing gradients of adhesivity along a specific embryonic axis might be resolved by active cell movements into oriented tissue extension (Gergen et al., 1986; Irvine and Wieschaus, 1994; Mittenthal and Mazo, 1983; Nardi and Kafatos, 1976a; Nardi and Kafatos, 1976b; Wieschaus et al., 1991).

Second, interactions with surrounding tissues during morphogenesis could trigger or otherwise influence patterned cell behavior. For example, recent studies in *Xenopus* and *Fundulus* embryos suggest signals emanating from localized specific cell populations or tissue boundaries could propagate through cell populations and thereby polarize motile and adhesive behaviors within them (Domingo and Keller, 1995; Shih and Keller, 1992; Trinkaus, 1998; Trinkaus et al., 1992). Alternatively, local interactions occurring at tissue boundaries could bias the directionality of cell extension or movement, for example through contact-dependent inhibition or stabilization of protrusive behavior at planar tissue boundaries (Jacobson and Moury, 1995; Jacobson et al., 1986; Keller et al., 1989; Keller et al., 1992), or interactions with an oriented extracellular matrix at vertical tissue boundaries (Keller et al., 1991; Nakatsuji et al., 1982; Nakatsuji and Johnson, 1983; Shih and Keller, 1992).

Here, we exploit the relatively simple organization and development of the ascidian embryo to assess the relative

contributions of intrinsic morphogenetic properties and tissue interactions to patterning the cell movements that drive invagination and convergent extension of the notochord. During ascidian notochord formation, morphogenetic pattern emerges rapidly within a sheet of 40 cells, in an embryo having only 500 cells. The embryo's geometry remains relatively unchanged as this pattern emerges, and the simple stereotyped movements of cells within the notochord and surrounding tissues are well described (Miyamoto and Crowther, 1985; Munro and Odell, 2002; Nishida, 1987). In contrast to many other embryos wherein determination and regionalization of cell fates occurs simultaneously with morphogenesis, primary cell types and regional identities of embryonic ascidian cells are determined long before notochord cells rearrange (Kawaminani and Nishida, 1997; Nakatani and Nishida, 1994; Nishida, 1990; Nishida, 1992b; Nishida, 1993; Nishida, 1994; Nishida and Satoh, 1989; Nishikata et al., 1987; Whittaker, 1990). Moreover, it is easy to identify and manipulate notochord cells and each of the surrounding tissues at key stages.

We first document the intrinsic morphogenetic potential of notochord rudiments, isolated just after they have been determined at the 64-cell stage. We then describe the use of micromanipulation and confocal microscopy to assess the relative contributions of tissues that surround the notochord to the emergence of pattern within it.

MATERIALS AND METHODS

Animal collection and culture

We performed all experiments on *Boltenia villosa*. We collected and maintained adults, and obtained and cultured their embryos as described in the accompanying paper (Munro and Odell, 2002).

Cell isolation and microablation techniques

Fig. 1 schematizes the micromanipulations we performed. We isolated notochord rudiments and all other embryo fragments under a stereomicroscope using hand-held glass microneedles, pulled from micropipette glass (OD: 1.0 mm; ID: 0.7 mm; Drummond Scientific, Broomell, PA) on a Flaming-Brown micropipette puller (Model P-72; Sutter Instruments, San Francisco, CA), and mounted on shortened 5" pasteur pipettes. We dipped needles in 1% agar to prevent their sticking to and lysing cells. We isolated presumptive notochord blastomeres at the 64-cell stage when notochord precursors first become lineage restricted and studied only those specimens in which all 4 notochord precursor cells remained undamaged. We performed all other fragment isolations at mid-late gastrula stages. Each isolation entailed, at most, two cuts, whose sites of initiation were well defined with respect to the stereotyped positions of identifiable blastomeres (Fig. 1).

To make notochord/posterior cap recombinants, we isolated notochord fragments as described above and then cultured them in filtered sea water (FSW) until control embryos had reached the mid gastrula stage. We then prepared posterior caps from the control population. In these caps, the posterior mesoderm formed a natural cleft into which we pressed notochord fragments using gentle pressure with a hand held microneedle. We then allowed the two fragments to adhere for up to an hour before transferring them to a separate dish.

To ablate identified neural plate or endoderm precursors we first lysed them at the 64-cell stage using sharpened tungsten needles under a stereo dissecting microscope, then allowed dead cells to separate from the remaining embryo through one cell division round, and finally cleaned them away using a hand held microneedle prepared as described above. In all cases we conclusively verified the specific ablation of the desired cell population (see Results for details).

Time lapse analysis of dorsal anterior quadrants

To visualize cell shape changes over time in dorsal anterior quadrants, we used the fluorochrome Bodipy (488 nm excitation; Molecular Probes, Eugene Ore) which diffuses freely into living embryos and concentrates into yolk granules within the cytoplasm yielding a "negative" image of cell outlines in confocal thin sections (Cooper and Kimmel, 1998). We pre-incubated dorsal anterior quadrants for 60 minutes in a 100 μM solution of Bodipy in FSW, transferred them through several FSW rinses, and then mounted them between two coverslips within a custom temperature-controlled chamber, as described in the accompanying paper (Munro and Odell, 2002), on the stage of a Biorad MRC 600 LSCM on a Nikon upright microscope. We imaged embryos using the 488 nm line of a krypton-argon laser and a 25× Plan Neofluor multi-immersion lens (Carl Zeiss) adjusted for water immersion. We collected images at 10-minute intervals from each of several identified embryo fragments within a field. We used the minimal exposure required to obtain usable images. Under these conditions, the embryo fragments developed to the same extent as either Bodipy-labeled or unlabelled embryos cultured without fluorescent excitation in Petri dishes.

Histological analysis

The methods we used to fix embryo fragments, stain them with Bodipy-phalloidin and analyze them with confocal microscopy are essentially the same as those described elsewhere (Munro and Odell, 2002). For morphometric measurements, we mounted embryos in a mixture of 30% glycerol in PBS to avoid the shrinkage and distortion that alcohol dehydration causes.

Notochord extension index

To characterize the extent to which notochord rudiments formed normal notochords under different experimental conditions, we devised a notochord extension index (NEI) which varies between 0 and 1, and reflects both convergent extension within the notochord plate, and overall extension of the notochord plate along the AP axis. Notochord rudiments that did not change their aspect ratio at all received an NEI score of 0. Rudiments that exhibited the degree of extension seen in normal embryos at the end of stage II when formation of the cylindrical intermediate is completed, but in which no cell had come to span the entire circumference, received a score of 0.5. The NEI score then increased in direct proportion to the fraction of cells within the rudiment that had completed rearrangement (i.e. rearranged to span the entire circumference of the notochord rudiment); thus a rudiment in which half the cells had completed rearrangement received a score of 0.75, and one in which all cells had completed rearrangement received a score of 1.0. In no case have we ever observed a notochord rudiment in which some cells had completed rearrangement, but which had not extended to the degree seen at the end of stage II. Thus our NEI is well defined.

RESULTS

Notochord cells isolated after induction differentiate autonomously but fail to rearrange normally

The ascidian notochord arises from two distinct lineages: a primary lineage producing 32 cells, which derives from the anterior blastomeres A7.3 and A7.7 (and their bilateral partners), and a secondary lineage producing 8 cells, which derives from the posterior blastomeres B8.6 (and its bilateral partner; Fig. 1). We focus here on the primary lineage for which more is known and which, independently of the secondary lineage (see below), makes a perfectly organized notochord.

To determine how much of their normal developmental program ascidian notochord cells can express in the absence of

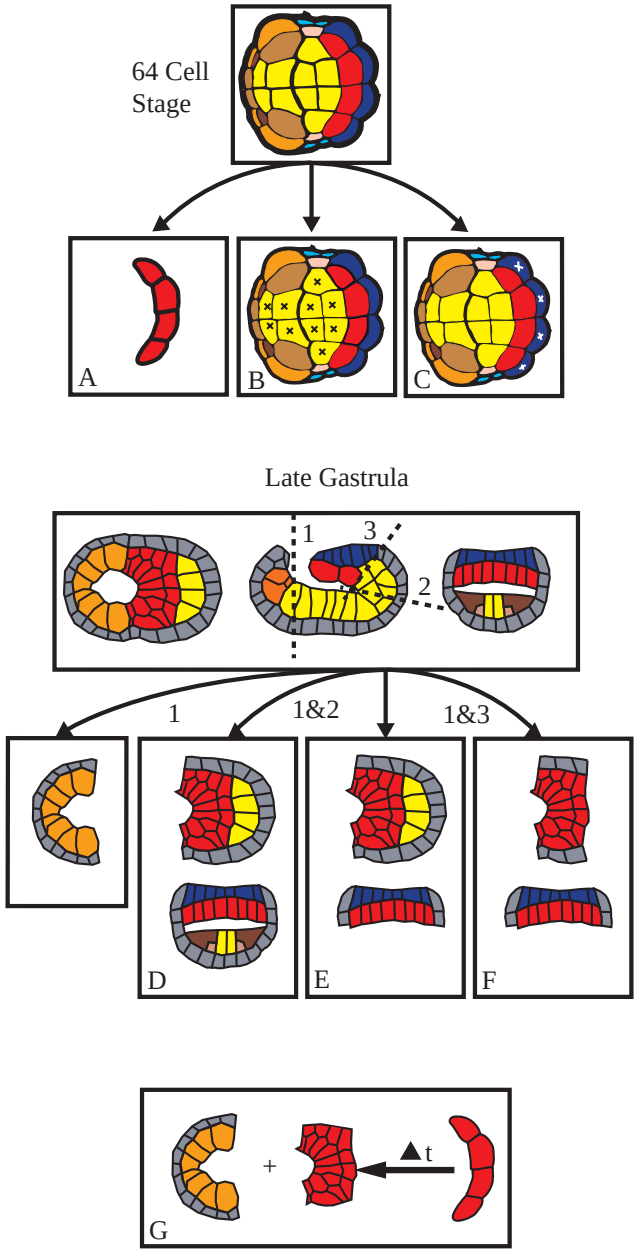

Fig. 1. An overview of the cut and paste experiments reported here. (A) Isolation of primary notochord precursors. (B) Endoderm ablation. (C) Ablation of neural plate precursors. (D) Isolation of anterior half embryos. (E) Isolation of dorsal anterior quadrants. (F) Co-isolation of notochord/notoplate. (G) Muscle/notochord recombination. Crosses in B and C indicate which blastomeres were ablated. The dashed lines 1-3 represent the positions of specific cuts made to obtain D-F.

surrounding tissues, we isolated primary notochord blastomeres at the 64 cell stage as a 4-cell rudiment consisting of blastomeres A7.3 and A7.7 and their bilateral partners (Fig. 1C), cultured them in filtered sea water (FSW) on non-adhesive coverslips, and monitored their development intermittently through a stereo microscope (n>100) or using time-lapse microscopy (n=8).

In normal embryos, cells of the primary notochord lineage divide three times: once just before the onset of gastrulation to form an arc of 8 cells; once at mid-gastrula stage along the AP axis; and again at the beginning of neurulation along the AP axis (Munro and Odell, 2002; Nishida, 1986). Just after the final notochord cell division, notochord cells within whole embryos become motile, and the notochord plate begins to converge and extend along, and invaginate about, the AP axis. Within six hours, they have achieved the stack of coins configuration.

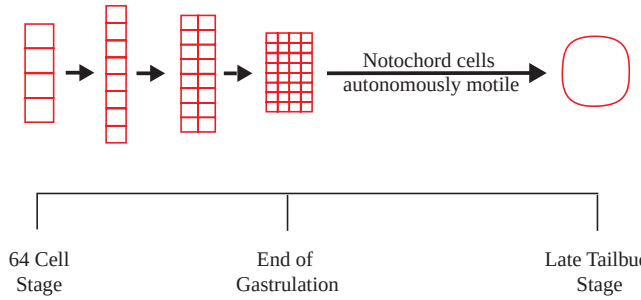

Fig. 2. Summary of morphogenetic behaviors expressed by primary notochord rudiments after their isolation at the 64-cell stage (see text for details).

Fig. 2 summarizes our observations of isolated notochord rudiments. In nearly all cases examined, notochord cells within isolated rudiments executed all three of their final divisions, with roughly normal timing relative to whole embryos cultured at the same temperature, giving rise to a full complement of 32 cells. Occasionally, one or two individual blastomeres began to divide at the appropriate time and then failed to complete their divisions. In some cases (<50%), non-adjacent blastomeres adhered to one another, disrupting normal neighbor relations within the notochord rudiment, and it was difficult to document the relative orientations of the two final notochord cell cleavages. But in every remaining case, normal neighbor relations were preserved, and the final two notochord cell cleavages occurred perpendicular to the axis of the first, as they do in situ. Thus by the end of the final notochord cell division, these rudiments had assumed proportions and a monolayer organization similar to that in normal intact embryos at the same time.

After their final division, notochord cells in isolated rudiments displayed local changes in shape, accompanied (in time-lapse movies) by the same type of local jostling behavior seen at similar stages in whole embryos (Miyamoto and Crowther, 1985; Munro and Odell, 2002). But no globally organized axis of cell shape change or rearrangement emerged in any isolated rudiment, nor did we ever observe invagination, or pronounced extension of the isolated notochord plate. Thereafter, notochord cells within isolated rudiments formed large intracellular vacuoles and swelled, much as their counterparts do in whole embryos (Cloney, 1964; Miyamoto and Crowther, 1985), or as isolated cells do when dissociated and cultured in calcium-free sea water (Nishida, 1992a).

Notochord cells within isolated rudiments express normal motility with normal timing

To assess the possibility that isolated notochord cells failed to express normal motile behaviors, we stained isolated notochord rudiments with Bodipy-phalloidin and used 3D confocal microscopy to characterize the occurrence, distribution and orientations of their F-actin-rich protrusions at selected stages. At mid-gastrula stage, F-actin organization was indistinguishable from that of notochord rudiments within

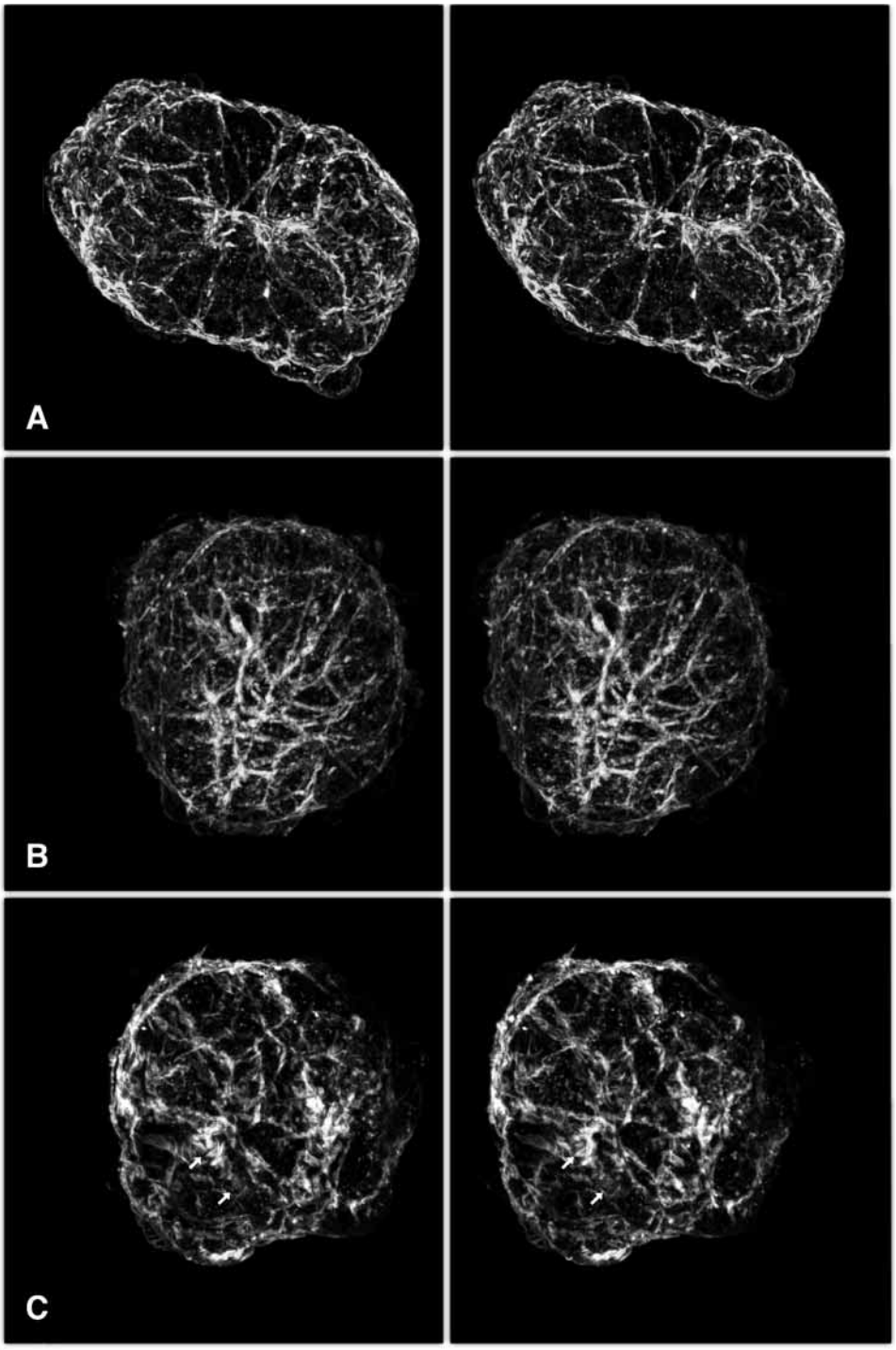

Fig. 3. Expression of F-actin-rich protrusions in isolated A-line notochord rudiments. Confocal sections were taken at 0.3 μm intervals through entire notochord rudiments and then made 3D reconstructions using NIH image. Each stereo pair was produced by combining two projections through the same confocal stack, in which the angle of the axis of projection differs by 6 degrees. (A) A 16-cell rudiment at the mid-gastrula stage. No localized protrusions can be seen. (B) By approximately 1 hour PFD, many cells bear detectable protrusions along interior edges. (C) At 3 hours PFD, protrusions are larger and more numerous, but no planar bias is evident.

intact embryos at the same stage, with no sign of the broader flattened protrusions characteristic of notochord cells during active rearrangement in situ (Fig. 3A). By 1 hour after the final notochord cell division (1 hour PFD), when cells in situ have begun to extend and rearrange, there was a pronounced general increase in the intensity of F-actin staining at interior edges and along many edges we could detect flattened F-actin rich protrusions, resembling those seen in intact embryos at the same stage (Fig. 3B). By 3 hours PFD, most interior notochord cell edges bore F-actin rich protrusions (Fig. 3C). These tended to be longer on average than those seen at 1 hour PFD as is the case for protrusions seen in situ at later stages. However, we could detect no obvious bias in the orientation of protrusions within the rudiment, in contrast to the in situ situation (Munro and Odell, 2002). These results suggest that cells in isolated notochord rudiments autonomously express the basic motile and adhesive machinery necessary to produce cell shape changes, but absent interactions with bounding tissues, these correct local behaviors produce no globally coherent result.

The role of bounding tissues in notochord formation

As the notochord rudiment forms an extended rod, it makes

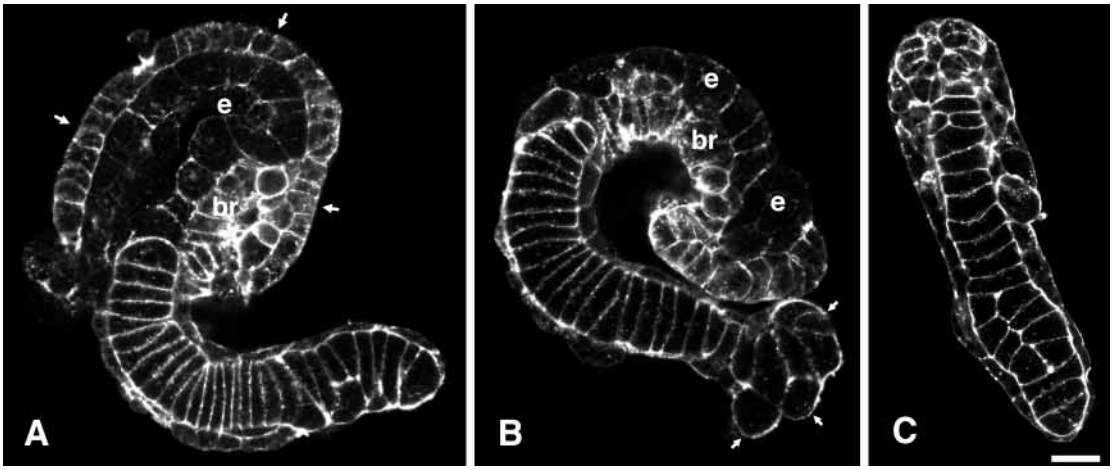

Fig. 4. Comparison of tadpole stages of (A) anterior half embryos, (B) dorsal anterior quadrants, and (C) notochord/neural plate coisolates. Posterior is bottom right in all three panels. e, endoderm; br, anterior neural tissue that normally gives rise to the brain; arrows in A indicate epidermis. Arrows in B indicate disorganized notochord cells that lost contact with an external substrate. In all three panels, the extended neural plate lies out of focus beneath the notochord. Scale bar, 10 μm.

contact with 4 distinct tissues (Fig. 1): presumptive anterior endoderm; lateral mesenchyme; presumptive neural plate and presumptive posterior muscle. We used a combination of co-isolation, microablation, and recombination techniques to assess the contributions that each of these tissues make to the emergence of morphogenetic pattern within the notochord (Fig. 1).

Posterior muscle and lateral mesenchyme are not necessary for notochord formation

To remove the influence of presumptive muscle, we ablated the entire posterior third of the embryo, leaving the notochord plate intact (Fig. 1D; n=54). The resulting 'anterior half embryos' extended small tails consisting of a central notochord, axial neural tissue, and a somewhat disorganized epidermis (Fig. 4A). To characterize the overall extent to which a normal notochord formed, we used a simple notochord extension index (NEI) (see Materials and Methods). For ventral half embryos, the NEI was 0.79±0.13, with an average 18/32 notochord cells spanning the entire notochord circumference. The best cases formed entirely normal notochords and the worst resembled the elongated cylindrical intermediates seen at late neurula stages (Munro and Odell, 2002). In general, notochords were most normal anteriorly and became more disorganized posteriorly.

In further experiments, we isolated 'dorsal anterior quadrants' containing only presumptive notochord, the overlying neural plate, anterior endoderm, and a few epidermal cells (Fig. 1E; n=37). The resulting embryoids (Fig. 4B) lacked the structures that normally form from ventrolateral cells, and somewhat fewer cells completed rearrangement, to span the entire notochord (NEI=0.65±0.08), but otherwise the results were the same as for ventral half embryos.

To look more closely at notochord formation in the absence of contact with mesoderm, we examined intermediate stages in living dorsal anterior quadrants using confocal microscopy with unconjugated Bodipy as a fluorescent label, to enhance contrast (Cooper and Kimmel, 1998). Mediolateral intercalation occurred with a time course similar to that seen in whole embryos (Fig. 5A-D). Cell shape changes tended to appear first in the anterior of the notochord plate and then spread posteriorly across the plate row by row (Fig. 6). We have observed this effect in some normal embryos (Munro and Odell, 2002), but it's much more robust here. Only the posteriormost notochord cells, which normally contact posterior muscle, failed to converge and extend or invaginate. These cells eventually lost contact with the overlying neural plate as the notochord rudiment extended and formed a disorganized mass of cells at the posterior of the extended notochord rod (see Fig. 4B).

As in whole embryos, the emergence of planar polarity was accompanied by a progressive invagination of the notochord plate (Fig. 5E,F). The overlying neural plate initially invaginated, but then adopted a downward curvature as the notochord plate invaginated (in the opposite direction) beneath it, with both neural plate cells and lateral epidermal cells becoming stretched as if passively deformed by invagination forces generated within the notochord plate (Fig. 5E,F).

Contact with neural plate alone is sufficient for the emergence of global polarity and notochord extension

To assess whether contact with neural plate alone is sufficient for the expression of normally polarized convergent extension and invagination, we co-isolated just the notochord rudiment and the overlying neural plate (Fig. 1F; n=40). In the resulting coisolates, notochords invaginated to form cylindrical intermediates (data not shown) and showed pronounced AP extension. However, rearrangement was less complete than in dorsal anterior quadrants (NEI=0.58±0.105), with no discernible difference in the degree of organization between anterior and posterior (Fig. 4C). In addition, at mid-neurula stages, both planar length/width ratios for individual cells, and AP extension of whole rudiments were significantly greater for dorsal anterior quadrants than for notochord/neural plate co-isolates (see Table 1). Thus, contact with neural plate alone is sufficient for both convergent extension and invagination, but contact with anterior endoderm may speed the emergence of planar polarity within the notochord plate, particularly at its anterior end (Fig. 6).

Embryos lacking presumptive endoderm gastrulate and form normal notochords

Previous studies have suggested that endoderm may act as a

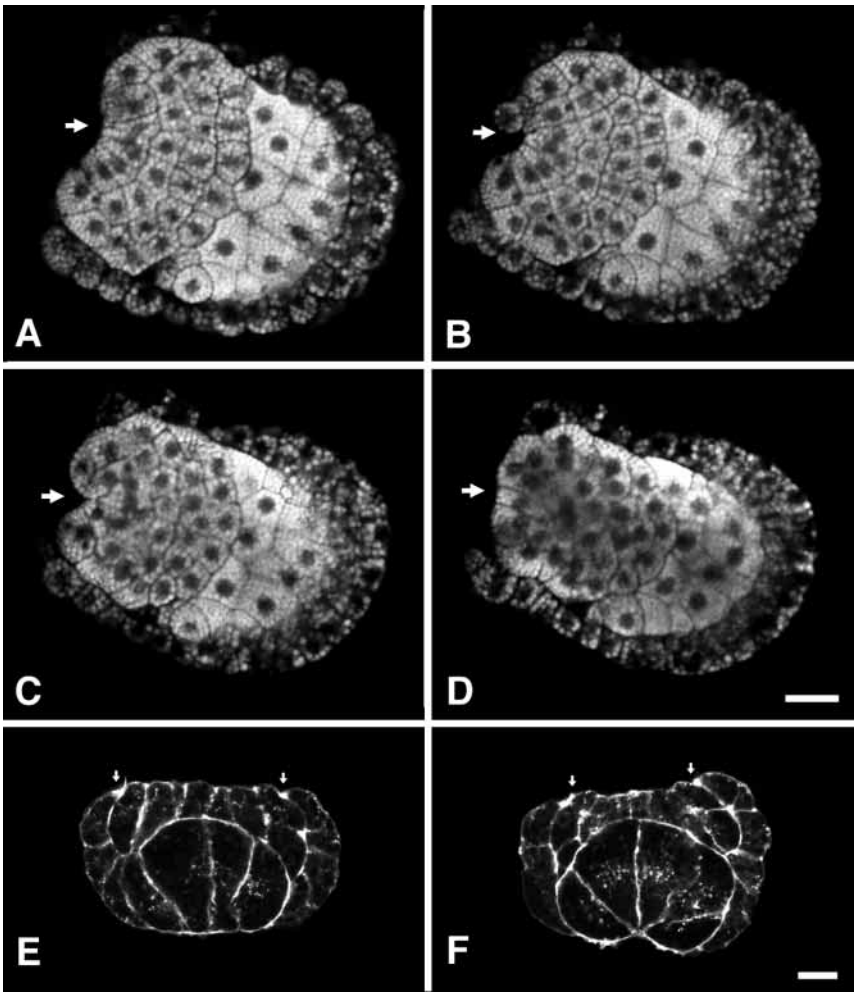

Fig. 5. Intermediate stages of notochord formation in dorsal anterior quadrants. (A-D) A dorsal anterior quadrant stained with Bodipy and imaged at (A)10 minutes, (B) 30 minutes, (C) 50 minutes, and (D) 70 minutes after completion of the final notochord cell division. Posterior is left in all panels. The larger cells to the right are anterior endoderm. The darker cells lining the edge are epidermal cells. The posterior-most notochord cells constrict their apices and many enter the interior of the notochord plate as they do during blastopore closure in whole embryos (arrows). But those that remain at the boundary never elongate or intercalate perpendicular to the AP axis. Scale bar, 20 μm. (E,F) Posterior (E) and anterior (F) cross-sectional views of dorsal anterior quadrants at approximately 3 hours PFD, when control embryos have completed formation of a cylindrical rod. Dorsal is up in both views. Arrows indicate the boundary between the neural plate and lateral epidermal cells. Note the downward curvature of the neural plate, which has normally closed to form a tube by this stage.

source of signals responsible for establishing cell fates (Nishida, 1996) and/or influencing gastrulation (Jeffery, 1992) of vegetally derived cells. This raised the possibility that signals from anterior endoderm between the 64 cell stage (when we isolated notochord rudiments) and mid-gastrula (when the experiments above show that anterior endoderm is dispensible) could set up a cryptic pre-pattern in notochord cells that emerges when they become motile. To rule out this possibility, we ablated all endoderm precursors (A7.1; A7.2; A7.5; B7.1; B7.2) at the 64-cell stage (Fig. 1A). In 16/16 cases, the resulting embryos formed and extended normal looking tails in which the organization of notochord and muscle appeared entirely normal (Fig. 7). Examination of intermediate stages revealed that the notochord primordium involuted normally despite the complete absence of a vegetal plate, and the notochord subsequently formed by convergence and extension along the normal AP axis via a cylindrical intermediate (data not shown). Thus, the emergence of morphogenetic pattern within the notochord plate does not require interactions with endodermal tissues any time after the 64-cell stage, nor does gastrulation of the notochord.

Embryos lacking notoplates make normal notochords, but by a very different route

To assess whether contact with neural plate is *necessary* for the emergence of morphogenetic pattern within the notochord plate, we ablated the precursors to the posterior neural plate (A7.4 and A7.8) at the 64-cell stage. In 44/47 of such cases, the notochord adopted a normal stack-of-coins configuration within tails that were normal except for the missing posterior neural tube (Fig. 8). We obtained a similar result when we also ablated the precursors of the anterior neural plate (data not shown).

To our surprise, we found that the notochord forms by a very different path in embryos lacking neural plates (Fig. 9). The notochord rudiment gastrulated normally, forming a plate of cells bounded anteriorly by presumptive endoderm but lacking the dorsal boundary that would normally be supplied by the posterior

Table 1. A comparison of length/width ratios for individual notochord cells and whole notochord rudiments at mid-neurula stage in dorsal anterior quadrants and notochord/neural plate co-isolates

Experiment no.	Type	L/W (cells)	L/W (rudiments)
1	DAQ	1.44±0.19 (*n*=11)	1.86±0.34 (*n*=53)
	NONP	1.17±0.13 (*n*=11)	1.68±0.42 (*n*=139)
2	DAQ	1.66±0.09 (*n*=9)	1.61±0.30 (*n*=131)
	NONP	1.31±0.14 (*n*=14)	1.38±0.23 (*n*=128)

Differences between DAQ and NONP are significant ($P<0.005$, Student's *t*-test) for all four comparisons.

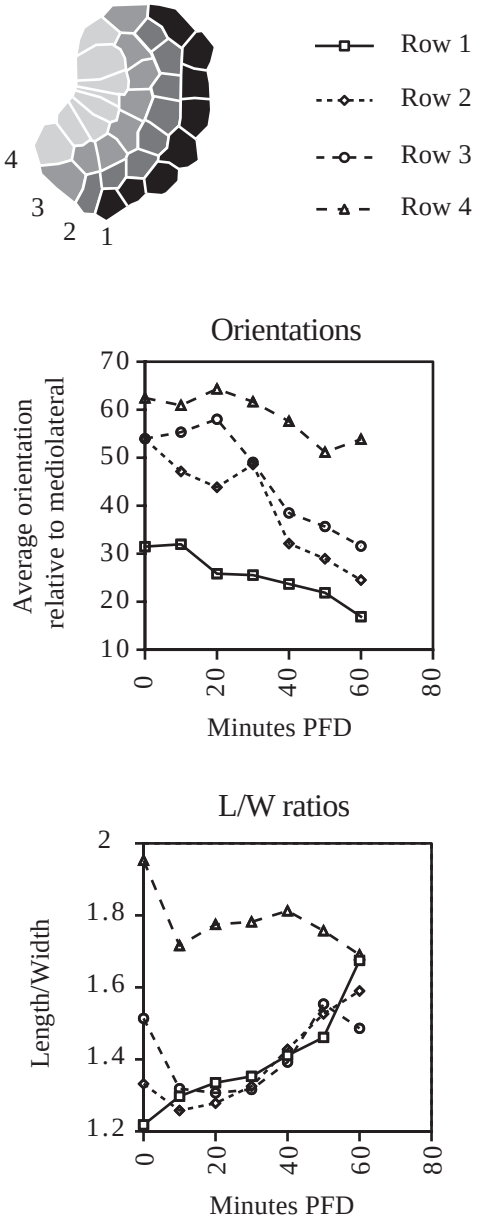

Fig. 6. Emergence of cell polarity in anterior half embryos. (A) Average cell orientation relative to the mediolateral axis of the notochord rudiment. Note the clear anterior-posterior progression in the emergence of a mediolateral orientation in rows 1-3, while cells in the posteriormost row do not become mediolaterally oriented. (B) The average length/width ratio of individual cells increases with a time course comparable to whole embryos. The initial decrease in L/W ratios for rows 2 and 3 reflect the fact that these cells are initially elongated *along* the AP axis of the embryoid and subsequently change their orientation by decreasing their cross-sectional extent along the AP axis and increasing it perpendicular to the AP axis in the same way that cells within intact embryos do (data not shown). Cells in the posterior-most row remain extended along the AP axis.

neural plate (data not shown). During its final division, the notochord rudiment condensed against the anterior endoderm and lateral epidermis, forming a monolayer sheet whose original mediolateral axis ran from the center of the anterior endoderm boundary to the lateral ends of the arc and whose original AP

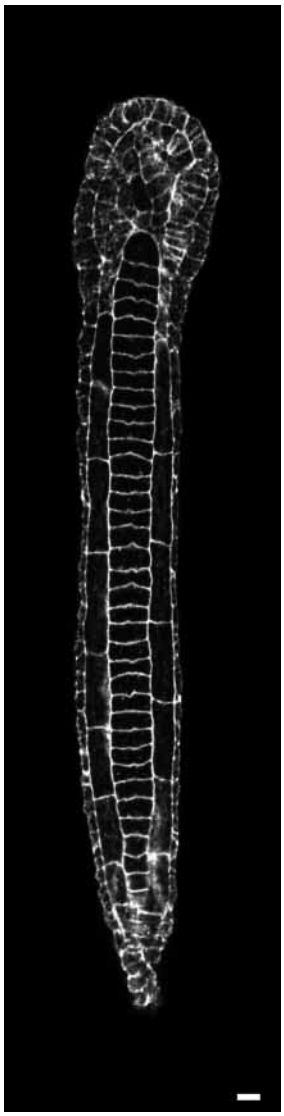

Fig. 7. Formation of a normal notochord in embryos lacking endoderm. Organization of the tadpole is essentially normal except for the absence of anterior gut structures. Scale bar, 10 μm.

axis was oriented dorsoventrally (Fig. 9A-C). During the next two hours, cells within the notochord plate elongated and intercalated dorsoventrally, *parallel* to the original AP axis instead of *perpendicular*, extending the lateral arms of the plate, which curved around posteriorly like arms of a drawn bow. (Fig. 9D-G). At the same time, each lateral arm invaginated about the axis of extension (arrow in Fig. 9G). Eventually, the two arms of the notochord plate met at the posterior midline and fused (Fig. 9E). Once initiated, this fusion zipped anteriorly along both the dorsal and ventral midlines (Fig. 9H), producing a cylindrical intermediate like those seen in normal embryos (Fig. 9I,J). Thereafter, the notochord elongated normally as cells intercalated around its circumference. Thus, the notochord cells achieved the same final configuration as in intact embryos, but they followed utterly different trajectories to get there.

Embryos lacking both neural plate and muscle do not form normal notochords

When we ablated posterior muscle in embryos lacking neural plates, early stages of notochord morphogenesis occurring up to about the mid-neurula stage (approx. 2 hours PFD) were essentially as described just above. Sometimes the extending

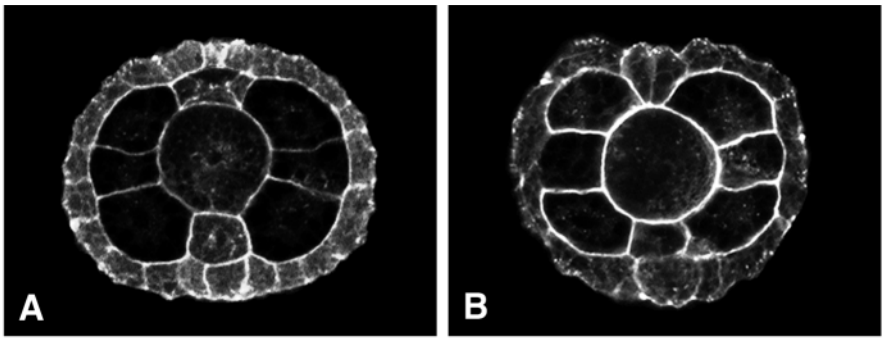

Fig. 8. Formation of normal notochords in embryos lacking the posterior neural plate (notoplate). (A) Control embryos; the axial neural tube can be seen in cross section as a set of four cells lying above the notochord and just below the dorsal epidermis. (B) Embryo lacking posterior neural plate. The axial neural tube is gone and instead a pair of epidermal cells contact the fully formed notochord along the dorsal midline.

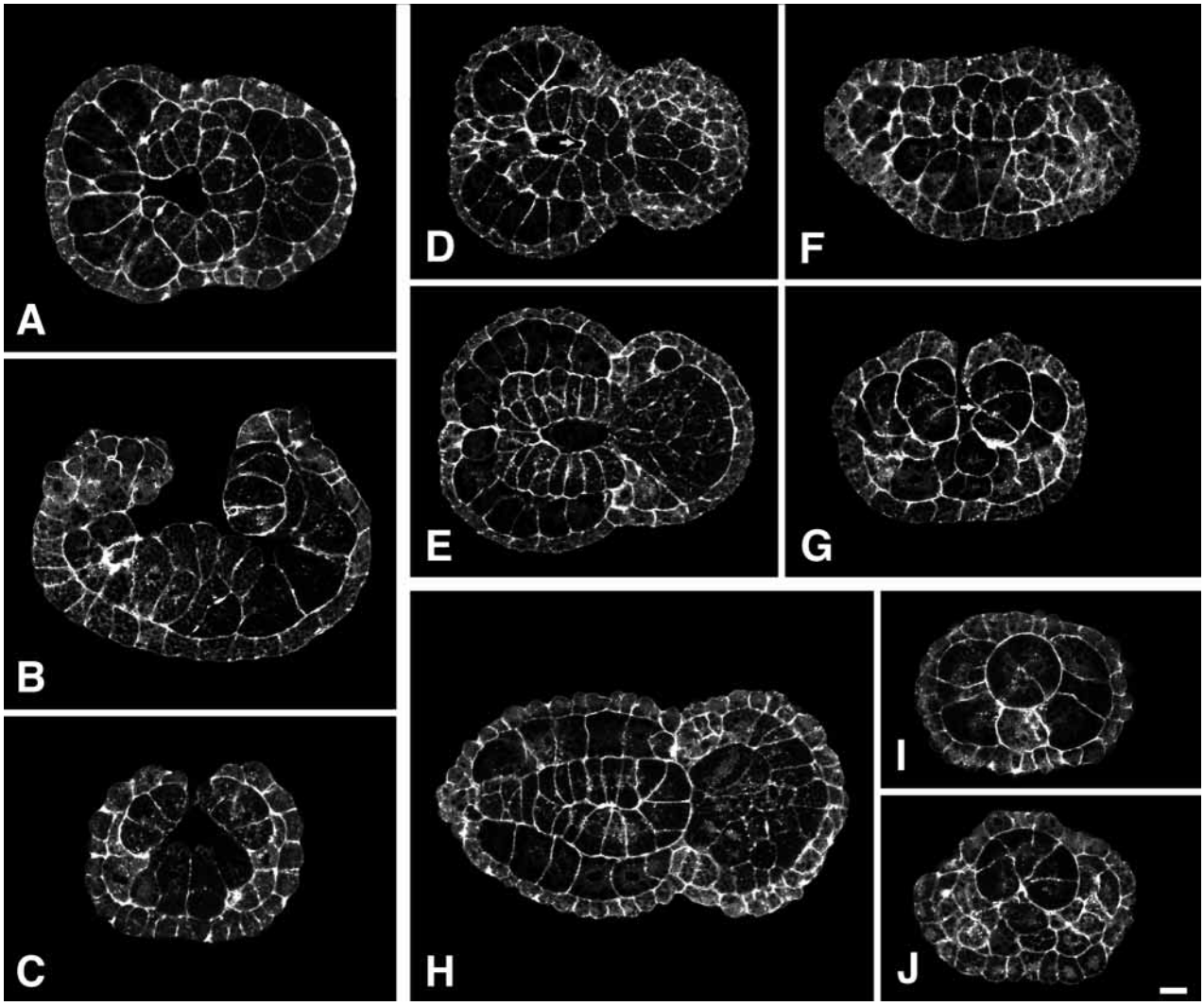

Fig. 9. Intermediate stages of notochord formation in embryos lacking the posterior neural plate. Posterior is left in all top and side views. Dorsal is up in all cross sections. (A-C) Approximately 1 hour PFD. (A) Top view. (B) Side view. (C) Cross section through the AP midline. Note that the anterior and lateral portions of the notochord remain a monolayer plate, but one that is oriented along the dorsal-ventral axis. The lateral epidermis and anterior endoderm now bound the basal surface of the notochord instead of the neural plate. (D-G) Approximately 2 hours PFD. (D) Dorsal top view. (E) Ventral top view. (F) Lateral section through one lateral arm of the notochord rudiment. (G) Cross section through the AP midline. Note the fusion of the two lateral notochord arms posteriorly (D) and the gradual posterior extension of the dorsal anterior boundary of the notochord plate (arrow in D) which is matched by a posteriorwards extension of the overlying epidermis (not shown). Note also the elongation of individual notochord cells perpendicular to the AP axis within the dorsal plate (D) and its lateral arms (F), and the constriction of cell apices within the lateral arms (arrows in G). (H-J) Approximately 3 hours PFD. (H) Top view. (I) Posterior cross section. (J) Anterior cross section. By this stage, the formation of a cylindrical intermediate is nearly complete. The organization of posterior muscle is essentially normal and the epidermis now bounds the notochord rod dorsally along its entire extent. Scale bar, 10 μm.

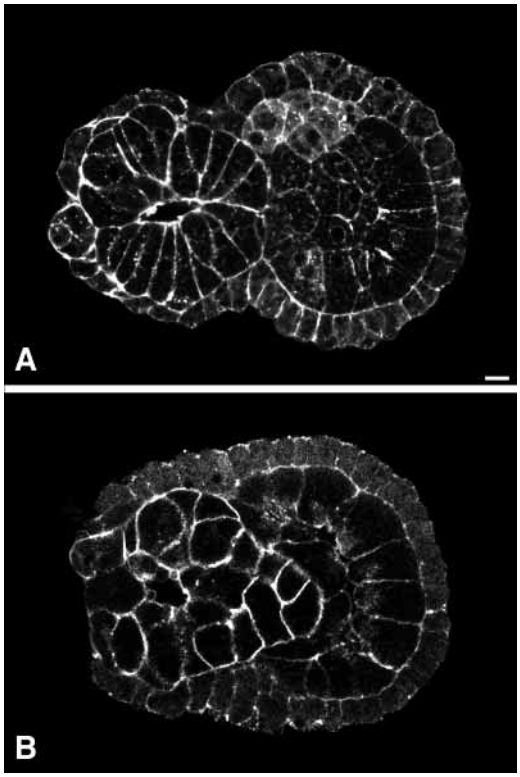

Fig. 10. Notochord fails to form a cylindrical intermediate in embryos lacking both neural plate and muscle. (A) Late neurula stage. The lateral notochord arms have met at the posterior (compare with D and E in Fig. 9). (B) Late tailbud stage. Individual notochord cells have begun to swell as they do at later stages in control embryos, but the overall shape and organization of the notochord rudiment remains similar to that seen at late neurula stage.

lateral arms of the notochord plate met posteriorly (Fig. 10A), but they invariably failed to anneal, remaining roughly the same length until the end of stage III when vacuolation and swelling of individual notochord cells caused it to extend somewhat (Fig. 10B). Thus, in the absence of neural plate, posterior muscle is necessary for the completion of notochord formation.

Notochord rudiments recombined with posterior fragments at late gastrula stage can form elongated cylindrical rods

To investigate whether contact with muscle cells is sufficient for the formation of an extended cylindrical rod, we isolated notochord rudiments, cultured them until controls had reached the late gastrula stage, and then recombined them, in random orientation, with posterior caps isolated at late gastrula stage (Fig. 1G), which consisted of an inner cup-shaped layer of presumptive muscle surrounded by an outer layer of presumptive epidermis and sometimes a few endodermal strand precursors.

In normal embryos, muscle cells rearrange during the first 3 hours PFD from a cap of cells 6 high and 6 wide to form an arc of cells 3 high and 12 wide that extends anteriorly along either side of the presumptive midline (Munro and Odell, 2002). Thereafter, all muscle cells elongate as the entire tail extends. In isolated posterior caps (without notochord), muscle cells rearranged normally during the first several hours, and the caps increased in length by a factor of 2.1±0.15, n=17), but the muscle cells did not subsequently elongate, so that at late tailbud stage the posterior cap remained short and stubby relative to normal tails (Fig. 11A). In notochord/posterior cap recombinants, notochord rudiments showed little shape change during the first several hours as the muscle cells rearranged and the caps elongated (data not shown). But thereafter, notochord rudiments extended along the AP axis defined by the posterior cap regardless of their initial orientation (NEI=0.66±0.1; n=24), accompanied by AP elongation of muscle cells and an increase in overall length of recombinant embryoids by a factor of 3.25 (±0.48; n=24). In the best cases, they formed recognizable tails with a central notochord flanked by parallel rows of extended muscle cells (Fig. 11B). While we did not directly confirm that notochords formed by convergent extension and invagination, cross-sectional views of recombinant embryos at tailbud stage revealed the typical cylindrical morphology and pizza-slice shaped cells seen in normal embryos during later phases of extension (not shown).

DISCUSSION

Isolated notochord rudiments express normal local morphogenetic behaviors, but do not make a notochord

Previous studies showed that primary notochord fates are specified by an inductive signal received at the 32-cell stage by the blastomeres A6.2 and A6.4, shortly before they divide to give rise to founders of the primary notochord (blastomeres

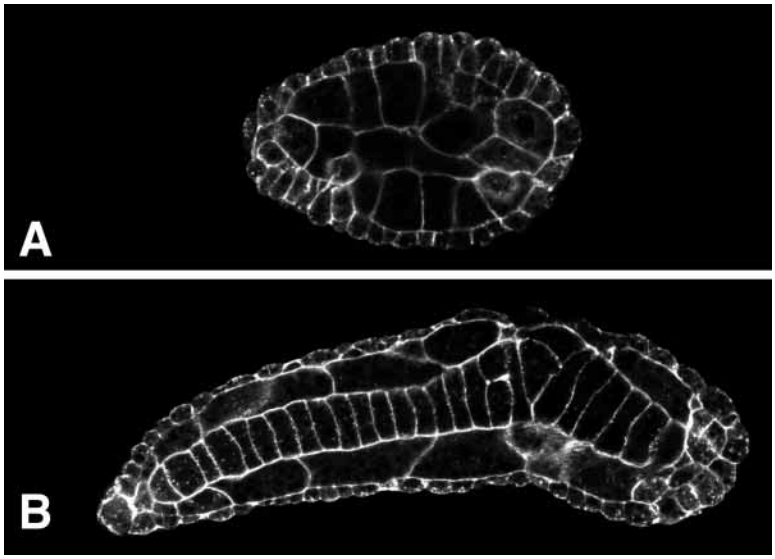

Fig. 11. Notochord extension in notochord/posterior cap recombinants. (A) Lateral view of a posterior cap cultured in isolation until the tailbud stage. Posterior muscle cells have rearranged to form (approximately) three rows of six cells each arrayed along either side of the axial midline. But individual muscle cells do not extend along the AP axis. (B) Notochord/posterior cap recombinant at the same stage. The notochord has extended with respect to the AP axis of the posterior cap and individual muscle cells are considerably elongated along the AP axis. Scale, 10 μm.

A7.3 and A7.7) and posterior neural plate (A7.4 and A7.8) lineages (Nakatani and Nishida, 1994; Nakatani and Nishida, 1997; Nakatani et al., 1996). Here, we show that this early induction (and a maternal endowment) is sufficient to specify a normal sequence of cell divisions culminating in the formation of a notochord plate, and the normally timed expression of basolateral protrusive behaviors, indistinguishable from those observed in whole embryos. But in the absence of all contacts with surrounding tissues, neither localized protrusive activity nor local cell shape change become biased with within the plane of the epithelium or along its apicobasal axis, and rudiments neither converge and extend nor invaginate. Thus normal notochord morphogenesis must depend on an interplay between motile behaviors expressed autonomously within the notochord plate, and interactions with neighboring tissues that somehow bias these behaviors or constrain the forces they produce to achieve a globally patterned result.

Convergent extension and invagination are robust properties of the notochord plate, expressed whenever minimal conditions are met

To our surprise, we find that none of the tissues normally bounding the notochord are required for it to form an extended invaginated rod. Basal contact with neural plate OR posterior muscle OR anterior endoderm/lateral mesenchyme is sufficient. Planar contact with anterior endoderm, while not alone sufficient, enhances the response to neural plate alone. Furthermore, each of these interactions can determine a different axis of invagination/convergent extension relative to the original AP axis of the embryo (Fig. 12): in normal contact with neural plate with or without endoderm, the notochord extends AP as in normal embryos. In embryos lacking neural plate, the notochord plate invaginates and extends *perpendicular* to the embryonic AP axis. In notochord/muscle recombinants, the notochord extends along the axis defined by the posterior muscle, regardless of its original axis.

Together, these data suggest that the notochord plate has a robust intrinsic tendency to converge and extend along, and invaginate about, *some* axis so long as minimal requirements are met, but *which* axis can be determined by cues supplied by specific contacts with neighboring tissues. The notochord plate may have an intrinsically preferred axis, but if so, it can be readily overridden by interactions with neighboring tissues. Furthermore, at least three of these interactions occur during normal notochord formation in such a way that the cues they supply could act redundantly or synergistically to specify the correct axis of invagination and convergent extension. Our data also support the idea, suggested by our descriptive work (Munro and Odell, 2002), that the cellular mechanisms underlying invagination and convegent extension must be closely coupled, for we never observe one without the other under any experimental condition.

What are the minimal sufficient requirements for invagination and convergent extension to occur? One may be the polarizing cue discussed above, although we cannot rule out the possibility that the notochord plate has a weak intrinsic polarity, which external cues override. The other is almost certainly basal contact with an external tissue substrate. Each of the sufficient interactions listed above meets this condition, and notochord cells that lose basal contact with an underlying substrate lose (or never gain) planar and epithelial polarity, even when they retain planar contact with adjacent notochord cell

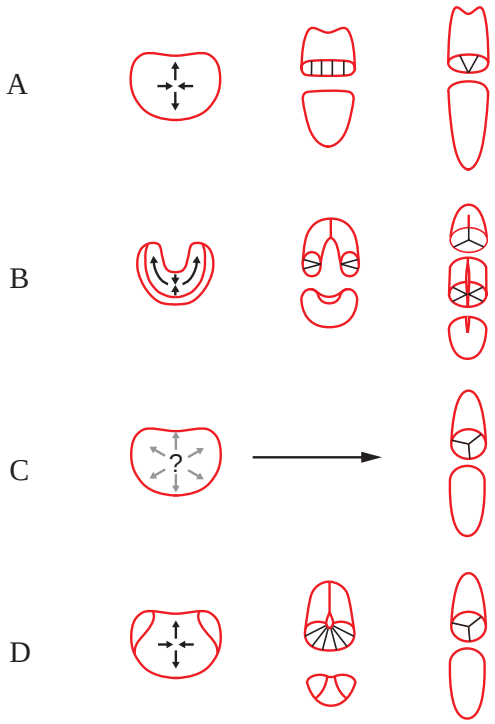

Fig. 12. Different modes of ascidian notochord formation. In notochord/neural plate co-isolates (and dorsal anterior quadrants) (A), basal contact with neural plate (and planar contact with anterior endoderm) specify convergent extension along and invagination about the embryonic AP axis. In embryos lacking neural plates (B), basal contact with anterior endoderm and/or lateral mesenchyme and/or epidermis specifies invagination/extension along a perpendicular axis. The extending lateral arms subsequently meet at the posterior and then re-anneal along the embryonic midline. In notochord/posterior cap recombinants (C), contact with posterior muscle specifies formation and extension of a cylindrical rod along the AP axis of the posterior cap, regardless of the initial orientation of the notochord rudiment. In normal embryos (D) multiple tissue interactions redundantly specify and support the normal mode of convergent extension and invagination.

neighbors (see e.g. Fig. 4B and Fig. 5A-D). However, planar contact with neural plate or anterior endoderm, in the absence of any other basal contact, does not induce or support globally organized convergent extension and invagination of notochord rudiments (data not shown), even though basal contacts with the same tissues do, and even though planar contact with anterior endoderm alone can induce *locally* polarized convergent extension (data not shown). Thus basal contact with an external tissue is almost certainly a necessary condition, and basal contact plus a polarizing cue is probably sufficient. Presumably basal contact with neural plate, posterior muscle, and anterior endoderm/lateral mesenchyme are each sufficient because they supply basal support and a polarizing cue. Whether basal contact with *any* adhesive substratum (e.g. an artificial one), coupled to a polarizing cue, would suffice remains to be seen.

Mechanisms for the establishment of global polarity

How basal contacts and planar polarization cues interact with notochord cells to produce invagination and convergent extension is unclear. However, it seems likely that they act by aiming autonomously expressed basolateral extension within the plane

of the notochord plate and along its apical-to-basal axis in a particular direction so as to produce convergent extension and invagination respectively. In the companion paper (Munro and Odell, 2002), we hypothesize that local attempts of basolateral notochord cell edges to extend are opposed by cortical forces that attempt to contract the cell boundary about a constant cytoplasmic volume. This results in a tug-of-war in which basolateral edges compete for a limited cell volume, with winning edges extending and losers retracting. In this context, any number of mechanisms could act either locally or globally to bias the outcome of this competition. Basal contact with an external tissue could provide the apico-basal bias either indirectly by providing an external cue necessary for the maintenance of general epithelial polarity and the polarized deployment of force-generating cytoskeletal machinery, or more directly by providing an adhesive contact that retards active contraction of basal notochord cell surfaces relative to apical ones. Alternatively, it may operate in more subtle ways to allow the coordination and or spread of planar polarity within the notochord monolayer.

With regard to planar polarization, diffusible signals arising at junctions between different tissues could influence the frequency or strength of local protrusions (Domingo and Keller, 1995; Shih and Keller, 1992). Local contact inhibition of protrusive activity or adhesive stabilization of local cell extensions at tissue boundaries could favor protrusive extension away from those boundaries (Jacobson and Moury, 1995; Jacobson et al., 1986; Keller et al., 1989; Shih and Keller, 1992). Cell extensions might be selectively stabilized along a particular axis through basal contact with an oriented extracellular matrix (Nakatsuji et al., 1982; Nakatsuji and Johnson, 1983; Weiss, 1945) or through interaction with an adhesive gradient (Poole and Steinberg, 1982). Finally, our own modeling studies (E. M. M. and G. O., unpublished) suggest a number of mechanical and geometric effects, mediated through adhesive contacts with surrounding tissues, that could provide the necessary cues.

Mechanical integration of local polarity cues within the notochord rudiment

Regardless of what these cues are, their combined effect must be determined by how they are integrated through local cell-cell interactions within the notochord. In a close packed tissue, any interior edge, in order to extend, must displace neighboring cells. Neighboring cell edges attempting to extend at right angles to one another will compete for the same tissue volume while those attempting to extend in parallel will synergize in their efforts. This simple mechanical observation has several important implications: First, locally established polarity will tend to propagate across a monolayer (Weliky et al., 1991) consistent with what we have observed in dorsal anterior quadrants (Fig. 5) and with what others have described elsewhere (Domingo and Keller, 1995; Shih and Keller, 1992). Secondly, competing orientation biases arising at different local positions, either within the notochord or along its boundary, will be resolved at any given point in a field of cells as a compromise orientation, weighted by the relative strengths of those biases (Elsdale and Bard, 1972). Resolving forces and cell volume conservation globally provides a general mechanism that converts orientation biases arising at different locations and by different mechanisms into a common currency, integrated across the notochord to produce a global result. This provides a satisfying explanation for the robustness with which the correct orientation emerges, since, in this common currency, one cue can readily substitute for another, and adding additional cues only enhances the overall reliability of the process. Indeed, from this perspective, it is not surprising that many independent cues might have arisen during evolution.

Regulative mechanisms of notochord formation

We were surprised to observe a completely different mode of notochord formation in embryos lacking neural plates. In this case, invagination and convergent extension along an axis perpendicular to the normal axis drives the formation of a U-shaped rudiment which must subsequently regulate to form a normally oriented cylindrical rod; and this regulation fails to occur when posterior muscle is absent. To complete formation of a cylindrical rod, both free edges of each lateral arm must meet and anneal at the midline both dorsally and ventrally, but this is exactly what happens ventrally, in normal embryos. Since notochord cells clearly have a mutual adhesive affinity, we would expect these edges to fuse if brought into sufficiently close contact. From this perspective, the contribution of posterior muscle may be: (a) to provide a narrow channel which forces lateral arms together as they coextend into it; and (b) to provide an external substrate that coextends with the notochord rudiment providing the basal support necessary for notochord cells to maintain planar and epithelial polarity. In the absence of this support, notochord cells would lose basal contact as the lateral arms extended and become disorganized.

Another regulative aspect of notochord formation revealed by our experiments is an intrinsic tendency for the notochord rudiment to adopt a uniformly circular cross section despite any differences in its initial shape and the shapes and mechanical properties of the tissues it contacts. These observations imply that the forces that generate uniform circularity reside within the notochord plate itself. The simplest explanation, consistent with our observations and the mechanical framework outlined above (and in Munro and Odell, 2002) is this. The same cortical contractile forces that cause a single cell to round up, or make all cells in a sheet isodiametric, will force a flat sheet of cells to form a circular disk, and a solid mass of cells or a hollow epithelial cyst to become spherical mass. At the same time, active convergent extension forces drive extension of the notochord rudiment along a single axis and thus the preferred shape becomes a circular cylinder.

Evolutionary implications

These observations have important implications for the evolution of notochord formation and function within the chordate phylum. The cylindrical rod form of an ascidian embryo's notochord is a characteristic intermediate stage in all chordate embryos examined thus far (Bancroft and Bellairs, 1976; Brun and Garson, 1984; Conklin, 1928; Keller et al., 1989; Lofberg, 1974; Sulik et al., 1994; Wood and Thorogood, 1994). However the *way* notochord cell precursors collectively arrive at this stage, the embryonic context in which they do so, and the subsequent elaboration and ultimate fate of the notochord rudiment, differs considerably from one organism to the next. If the intrinsic robustness with which this structure forms in ascidians were a conserved characteristic of the notochord lineage, it would help to explain its persistence in the face of divergent developmental origins and fates.

Ed Munro wishes to thank Victoria Foe, Bill Moody and the members of his lab for sharing lab space, equipment and reagents during the course of this work. We thank Mark Cooper for his gift of fluorescent Bodipy, and Eli Meir, Billie Swalla and George von Dassow and anonymous reviewers for insightful comments on the manuscript. Ed Munro was supported by an NSF predoctoral fellowship, and a predoctoral training grant in molecular and cell biology from the NIH.

REFERENCES

Bancroft, M. and Bellairs, R. (1976). The development of the notochord in the chick embryo, studied by scanning and transmission electron microscopy. *J. Embryol. Exp. Morphol.* **35**, 383-401.

Brun, R. B. and Garson, J. A. (1984). Notochord formation in the mexican salamander (*Ambyostoma mexicanum*) is different from notochord formation in *Xenopus laevis*. *J. Exp. Zool.* **229**, 235-240.

Cloney, R. A. (1964). Development of the ascidian notochord. *Acta Embryol. Morphol. Exp.* **7**, 111-130.

Conklin, E. G. (1928). The embryology of amphioxus. *J. Morphol.* **54**, 69-151.

Cooper, M. S. and Kimmel, C. B. (1998). Morphogenetic cell behaviors and specification of cell fate during early teleost development. In *Motion Analysis of Living Cells* (ed. D. Soll), pp. 177-220. New York: Wiley-Liss.

Domingo, C. and Keller, R. (1995). Induction of notochord cell intercalation behavior and differentiation by progressive signals in the gastrula of *Xenopus laevis*. *Development* **121**, 3311-3321.

Elsdale, T. and Bard, J. (1972). Cellular interactions in mass cultures of human diploid fibroblasts. *Nature* **236**, 152-155.

Gergen, J. P., Coulter, D. and Wieschaus, E. (1986). Segmental pattern and blastoderm cell identities. *Symp. Soc. Dev. Biol.* **43**, 195-220.

Irvine, K. D. and Wieschaus, E. (1994). Cell intercalation during Drosophila germband extension and its regulation by pair-rule segmentation genes. *Development* **120**, 827-841.

Jacobson, A. G. and Moury, J. D. (1995). Tissue boundaries and cell behavior during neurulation. *Dev. Biol.* **171**, 98-110.

Jacobson, A. G., Oster, G. F., Odell, G. M. and Cheng, L. Y. (1986). Neurulation and the cortical tractor model for epithelial folding. *J. Embryol. Exp. Morphol.* **96**, 19-49.

Jeffery, W. R. (1992). A gastrulation center in the ascidian egg. *Development* **Suppl.** 53-63.

Kawaminani, S. and Nishida, H. (1997). Induction of trunk lateral cells, the blood cell precursors, during ascidian embryogenesis. *Dev. Biol.* **181**, 14-20.

Keller, R., Cooper, M. S., Danilchick, M., Tibbetts, P. and Wilson, P. A. (1989). Cell intercalation during notochord formation in *Xenopus laevis*. *J. Exp. Zool.* **251**, 134-154.

Keller, R., Shih, J. and Domingo, C. (1992). The patterning and functioning of protrusive activity during convergence and extension of the Xenopus organiser. *Development Suppl.* 81-91.

Keller, R., Shih, J. and Wilson, P. (1991). Cell motility, control and function of convergence and extension during gastrulation in *Xenopus*. In *Gastrulation. Movements, Patterns, and Molecules*, vol. 1 (ed. R. Keller, J. Wallis H. Clark and F. Griffen), pp. 101-120. New York and London: Plenum Press.

Lofberg, J. (1974). Apical surface topography of invaginating and non-invaginating cells. a scanning-transmission study of amphibian neurulae. *Dev. Biol.* **36**, 311-329.

Mittenthal, J. E. and Mazo, R. M. (1983). A model for shape generation by strain and cell-cell adhesion in the epithelium of an arthropod leg segment. *J. Theor. Biol.* **100**, 443-483.

Miyamoto, D. M. and Crowther, R. J. (1985). Formation of the notochord in living ascidian embryos. *J. Embryol. Exp. Morphol.* **86**, 1-17.

Munro, E. M. and Odell, G. M. (2002). Polarized basolateral cell motility underlies invagination and convergent extension of the ascidian notochord. *Development* **129**, 13-24.

Nakatani, Y. and Nishida, H. (1994). Induction of notochord during ascidian embryogenesis. *Dev. Biol.* **166**, 289-299.

Nakatani, Y. and Nishida, H. (1997). Ras is an essential component for notochord formation during ascidian embryogenesis. *Mech. Dev.* **68**, 81-89.

Nakatani, Y., Yasuo, H., Satoh, N. and Nishida, H. (1996). Basic fibroblast growth factor induces notochord formation and the expression of As-T, a Brachyury homolog, during ascidian embryogenesis. *Development* **122**, 2023-2031.

Nakatsuji, N., Gould, A. C. and Johnson, K. E. (1982). Movement and guidance of migrating mesodermal cells in Ambystoma maculatum gastrulae. *J. Cell. Sci.* **56**, 207-222.

Nakatsuji, N. and Johnson, K. E. (1983). Conditioning of a culture substratum by the ectodermal layer promotes attachment and oriented locomotion by amphibian gastrula mesodermal cells. *J. Cell Sci.* **59**, 43-60.

Nardi, J. B. and Kafatos, F. C. (1976a). Polarity and gradients in lepidopteran wing epidermis. I. Changes in graft polarity, form, and cell density accompanying transpositions and reorientations. *J. Embryol. Exp. Morphol.* **36**, 469-487.

Nardi, J. B. and Kafatos, F. C. (1976b). Polarity and gradients in lepidopteran wing epidermis. II. The differential adhesiveness model: gradient of a non-diffusible cell surface parameter. *J. Embryol. Exp. Morphol.* **36**, 489-512.

Nishida, H. (1986). Cell division pattern during gastrulation of the ascidian, *Halocynthia roretzi*. *Dev. Growth Differ.* **28**, 191-201.

Nishida, H. (1987). Cell lineage analysis in ascidian embryos by intracellular injection of a tracer enzyme. III. Up to the tissue restricted stage. *Dev. Biol.* **121**, 526-541.

Nishida, H. (1990). Determinative mechanisms in secondary muscle lineages of ascidian embryos: development of muscle-specific features in isolated muscle progenitor cells. *Development* **108**, 559-568.

Nishida, H. (1992a). Developmental potential for tissue differentiation of fully dissociated cells of the ascidian embryo. *Roux's Arch. Dev. Biol.* **201**, 81-87.

Nishida, H. (1992b). Regionality of egg cytoplasm that promotes muscle differentiation in embryo of the ascidian *Halocynthia roretzii*. *Development* **116**, 521-529.

Nishida, H. (1993). Localized regions of egg cytoplasm that promote expression of endoderm-specific alkaline phosphatase in embryos of the ascidian *Halocynthia roretzi*. *Development* **118**, 1-7.

Nishida, H. (1994). Localization of egg cytoplasm that promotes differentiation to epidermis in embryos of the ascidian *Halocynthia roretzi*. *Development* **120**, 235-243.

Nishida, H. (1996). Vegetal egg cytoplasm promotes gastrulation and is responsible for specification of vegetal blastomeres in embryos of the ascidian *Halocynthia roretzi*. *Development* **122**, 1271-1279.

Nishida, H. and Satoh, N. (1989). Determination and regulation in the pigment cell lineage of the ascidian embryo. *Dev. Biol.* **132**, 355-367.

Nishikata, T., Mita, M.-I., Deno, T. and Satoh, N. (1987). Muscle cell differentiation in ascidian embryos analysed with a tissue-specific monoclonal antibody. *Development* **99**, 163-171.

Poole, T. J. and Steinberg, M. S. (1982). Evidence for a guidance of pronephric duct by a craniocaudally travelling adhesion gradient. *Dev. Biol.* **92**, 144-158.

Shih, J. and Keller, R. (1992). Patterns of cell motility in the organizer and dorsal mesoderm of *Xenopus laevis*. *Development* **116**, 915-930.

Sulik, K., Dehart, D. B., Iangaki, T., Carson, J. L. and Vrablik, T. (1994). Morphogenesis of the murinenode and the notochord plate. *Dev. Dyn.* **201**, 260-278.

Trinkaus, J. P. (1998). Gradient in convergent cell movement during Fundulus gastrulation. *J. Exp. Zool.* **281**, 328-335.

Trinkaus, J. P., Trinkaus, M. and Fink, R. D. (1992). On the convergent cell movements of gastrulation in Fundulus. *J. Exp. Zool.* **261**, 40-61.

Weiss, P. (1945). Experiments on cell and axon orientation *in vitro*: The role of colloidal exudates in tissue organization. *J. Exp. Zool.* **100**, 353-386.

Weliky, M., Minsuk, S., Keller, R. and Oster, G. (1991). Notochord morphogenesis in *Xenopus laevis*: simulation of cell behavior underlying convergence and extension. *Development* **113**, 1231-1244.

Whittaker, J. R. (1990). Determination of alkaline phosphatase expression in endodermal cell lineages of an ascidian embryo. *Biol. Bull.* **178**, 222-230.

Wieschaus, E., Sweeton, D. and Costa, M. (1991). Convergence and extension during germband elongation in *Drosophila* embryos. In *Gastrulation. Movements, patterns, and molecules*, vol. 1 (ed. R. Keller, J. Wallis H. Clark and F. Griffen), pp. 213-224. New York and London: Plenum Press.

Wood, A. and Thorogood, P. (1994). Patterns of cell behavior underlying somitogenesis and notochord formation in intact vertebrate embryos. *Dev. Dyn.* **20**, 151-167.